

# Excitonic Correlations in the Intermetallic Fe<sub>2</sub>VAl

Ruben Weht and W. E. Pickett

*Department of Physics, University of California, Davis CA 95616*

(March 20, 2018)

The intermetallic compound Fe<sub>2</sub>VAl looks non-metallic in transport and strongly metallic in thermodynamic and photoemission data. It has in its band structure a highly differentiated set of valence and conduction bands leading to a semimetallic system with a very low density of carriers. The pseudogap itself is due to interaction of Al states with the *d* orbitals of Fe and V, but the resulting carriers have little Al character. The effects of generalized gradient corrections to the local density band structure as well spin-orbit coupling are shown to be significant, reducing the carrier density by a factor of three. Doping of this nonmagnetic compound by 0.5 electrons per cell in a virtual crystal fashion results in a moment of 0.5  $\mu_B$  and destroys the pseudogap. We assess the tendencies toward formation of an excitonic condensate and toward an excitonic Wigner crystal, and find both to be unlikely. We propose a model in which the observed properties result from excitonic correlations arising from two interpenetrating lattices of distinctive electrons ( $e_g$  on V) and holes ( $t_{2g}$  on Fe) of low density (one carrier of each sign per 350 formula units).

## I. INTRODUCTION

The electronic behavior of Fe<sub>2</sub>VAl has recently been discovered to be highly unusual. [1] The resistivity increases by a factor of six from 400 K to 2 K (where  $\rho=3$  m $\Omega$  cm) characteristic of a non-metal, but other properties indicate metallic character. A sharp Fermi cutoff is observed in the photoemission spectrum, and the specific heat coefficient  $\gamma(T) \equiv C/T$  more than doubles below 6 K (to 12 mJ/mol K<sup>2</sup>). Ferromagnetism (FM) in the related compounds Fe<sub>3</sub>Al and Fe<sub>3</sub>Si and probable antiferromagnetism (AF) in Fe<sub>2</sub>VSi [2] suggests magnetic behavior may be responsible. The stoichiometric compound itself has no magnetic transition, although the alloy system Fe<sub>2+x</sub>V<sub>1-x</sub>Al and the isoelectronic system Fe<sub>2+x</sub>V<sub>1-x</sub>Ga [3,4] are ferromagnetic with a Curie temperature that extrapolates to zero as  $x \rightarrow 0^+$ . The behavior of  $\rho$  and  $C/T$  were suggested [1] as similar to those of heavy fermion metals, which would make it a candidate for a 3*d* based heavy fermion system. If the resistivity peaked and began to decrease below 2K (as happens for UBe<sub>13</sub>, for example) the resemblance would be closer; however, the observed value of  $\gamma=12$  mJ/mole-K<sup>2</sup> at 2 K is well below that of accepted heavy fermion materials. [5]

Although this compound falls within an alloy system where the V/Fe ratio can be varied continuously, indications are [1] that the properties noted above apply to the material near or at the stoichiometric limit of an ideal Heusler (L2<sub>1</sub>) structure compound. This structure type is based on an underlying bcc lattice of lattice constant  $a/2$ , with V at (0,0,0), Al at  $(\frac{1}{2}, \frac{1}{2}, \frac{1}{2})a$ , and Fe atoms at  $(\frac{1}{4}, \frac{1}{4}, \frac{1}{4})a$  and  $(\frac{3}{4}, \frac{3}{4}, \frac{3}{4})a$ , where  $a=5.761$  Å is the lattice constant of the resulting fcc compound. This structure is also that of Fe<sub>3</sub>Al, which has two inequivalent Fe sites. The Fe<sub>I</sub> site (which is the V site in Fe<sub>2</sub>VAl) has eight Fe neighbors in octahedral configuration, while while the Fe<sub>II</sub> site has four Fe and four Al neighbors. In Fe<sub>2+x</sub>V<sub>1-x</sub>Al the larger V atoms occupy the Fe<sub>I</sub> site

for  $x \leq 0$ . This trend is followed by all transition metal atoms to the left of Fe in the periodic table (Ti, V, Cr). [6]

Singh and Mazin [7] have reported local density functional results that indicate that Fe<sub>2</sub>VAl is a low carrier density, compensated semimetal.  $\Gamma$ -centered holes of Fe  $t_{2g}$  antibonding character are compensated by zone-edge X-point holes of V  $e_g$  character. Because the data cannot be interpreted simply in terms of degenerate, noninteracting carriers with this semimetallic band structure, Singh and Mazin suggest that the behavior is caused by strong spin fluctuations of Fe atoms on the V site, due to non-stoichiometry or to antisite defects.

In this paper we discuss other possible causes of the peculiar observed behavior, starting from the semimetallic band structure obtained in the local density approximation. We show that Al plays a crucial, but ultimately indirect, part in determining the electronic structure, and that the magnetic state is unusually sensitive to band filling. Based on a calculated carrier density of one electron and one hole for each 350 unit cells, we consider parameters related to a possible excitonic condensate or to an excitonic Wigner crystal. These exotic phases are not favored by the parameters. The character and density of the carriers, the structure of their sublattices, and the anticipated dielectric behavior suggest that dynamic correlations of excitonic character are candidates to account for the enhanced ‘metallic’ spectral density that is accompanied by decreasing conduction.

## II. METHOD OF CALCULATION

We have used the linearized augmented plane wave method [8] that utilizes a fully general shape of density and potential. Both the WIEN97 code [9] and the WM-NRL code [10] have been used on different aspects of the calculations. The lattice constant of 5.761 Å was used.

LAPW sphere radii ( $R$ ) of 2.00 to 2.30 a.u. were used in various calculations, and with very well converged basis sets no discernible effect of sphere radius size was found. Cutoffs of  $RK_{max}$  up to 8.6-8.9 provided well converged basis sets varying from 330 to more than 500 functions per primitive cell. Self-consistency was carried out on  $k$ -points meshes of around 200 points in the irreducible Brillouin zone ( $12 \times 12 \times 12$  and  $15 \times 15 \times 15$  meshes).

To assess the finer details of the predictions of density functional theory, we used two forms of generalized gradient corrected exchange-correlation functionals from Perdew and coworkers. [11] Gradient corrected functionals have been observed to give small but sometimes important corrections to the band structure in several compounds. Spin-orbit coupling was included in a second variation approach as formulated by MacDonald *et al.* [12]

### III. CALCULATIONAL RESULTS

#### A. LDA Band Structure

The band structure of  $\text{Fe}_2\text{VAl}$  is shown in Fig. 1. The crucial feature is a disjointedness between occupied valence bands and unoccupied conduction bands that is unusual in an intermetallic compound. There are twelve bands to be filled by the valence electrons. Interestingly, these lower twelve bands are disconnected from the remaining bands throughout the Brillouin zone. The result is not quite a gap but rather a deep minimum (pseudo-gap) in the density of states (DOS) precisely where the Fermi level ( $E_F$ ) falls. The density of states  $N(E_F)$  does not vanish because there is a very small overlap of a V-derived conduction band minimum, containing electron carriers at the three inequivalent X points, with a three-fold degenerate  $\Gamma_{25'}$  valence band maximum arising from Fe-derived holes.

The hole band at  $\Gamma$  is roughly 40%  $t_{2g}$  on each Fe atom and 15% V, with minor Al character. The electron pockets at X are V  $e_g$  states (with minor Al character), but Fe  $d$  character is forbidden by symmetry. The total and atom decomposed and projected DOS is shown in Fig. 2. The Al states (not shown) are repelled from a wide region including the Fermi level by the strong  $d-d$  bonding, as discussed by Singh and Mazin. This repulsion, and the apparent unimportance of the Al atom, leaves a network that can be pictured as V-centered cubic  $\text{VFe}_8$  clusters connected along all edges in an fcc arrangement. Contour plots of the holes and the electrons in a (110) plane that contains the nearest neighbor separations are shown in Fig. 3.

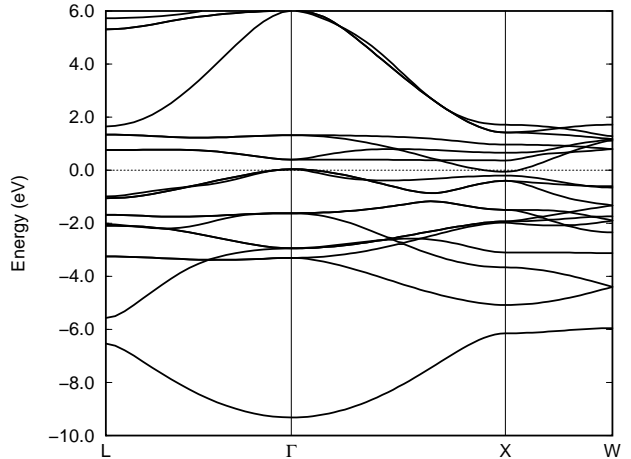


FIG. 1. Full band structure of  $\text{Fe}_2\text{VAl}$  along principle symmetry lines. The dashed line denotes the Fermi level. The lower band is  $s$ -like, primarily Al character. The Fe and V  $d$  bands lie between -5 eV and 2 eV.

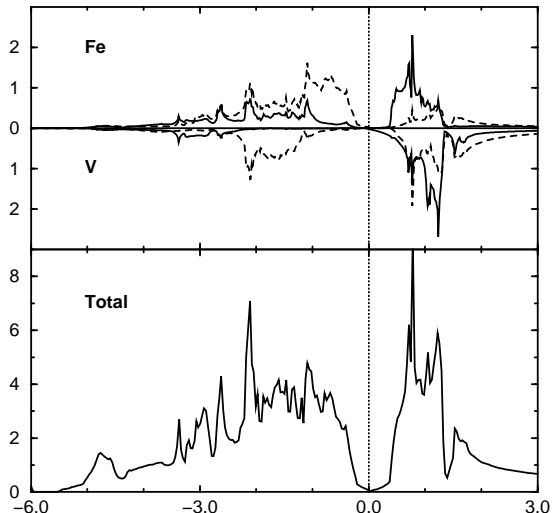


FIG. 2. Density of states of  $\text{Fe}_2\text{VAl}$  (bottom), projected onto the  $e_g$  (solid lines) and  $t_{2g}$  (dashed lines) crystal field characters of the Fe and V atoms (top of figure). The V density of states are plotted downward. Note that the Fermi level falls precisely in the minimum.

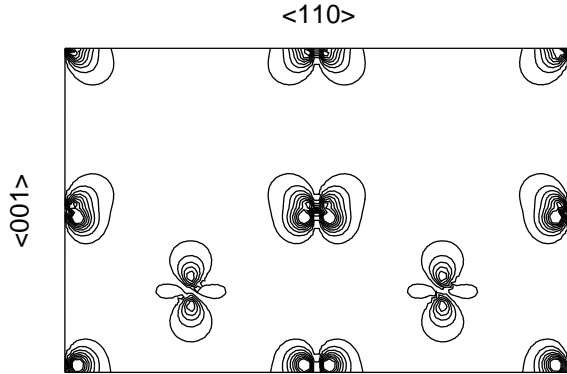


FIG. 3. Contour plot of the Fe-centered hole carriers (from the  $\Gamma$  point valence band maximum) and the  $e-g$  V-centered electron carriers (from the X point minimum) in  $\text{Fe}_2\text{VAI}$ , plotted in the (110) plane. Al atoms are centered in the empty regions. The separate densities were added to produce this figure. The  $t_{2g}$  type density on Fe (corners, edges, and center of the plot) looks normal when viewed in a (100) plane as is normally done.

The DOS shown in Fig. 2 is projected onto  $e_g$  and  $t_{2g}$  states on both Fe and V. The Fe  $t_{2g}$  states lie almost entirely below  $E_F$ , whereas the Fe  $e_g$  DOS is split into roughly equal amounts below and above the pseudogap. For V the  $e_g$  states lie entirely above the pseudogap, while the  $t_{2g}$  states form bonding-antibonding complexes separated across the gap by 3 eV.

The minimum direct gap of  $\approx 0.2$  eV occurs along the (100) directions near X. A “Penn gap” between the occupied and unoccupied DOSs, which gives a rough measure of where there is substantial absorption weight, would be at least 2 eV. The susceptibility of this system is discussed below.

## B. Gradient Corrections and Spin-Orbit Coupling

**Gradient Corrections.** The LDA band structure we obtain without gradient corrections and neglecting spin-orbit coupling is indistinguishable from that of Singh and Mazin. [7] Since the fine details are of interest in determining the predicted effective masses and carrier densities, we have calculated the generalized gradient corrections of Perdew and coworkers [11] and also included spin-orbit coupling. [12] The resulting bands are those shown in Fig. 1, and an enlargement near the Fermi level is pictured in Fig. 4. Gradient corrections lead to a shift of the X point conduction minimum upward with respect to the  $\Gamma$  point band maximum, by 95 meV. This reduces the band overlap (before spin-orbit coupling) from 200 meV to 100 meV, and reduces the number of carriers by

roughly  $(100/200)^{3/2} \approx \frac{1}{3}$ .

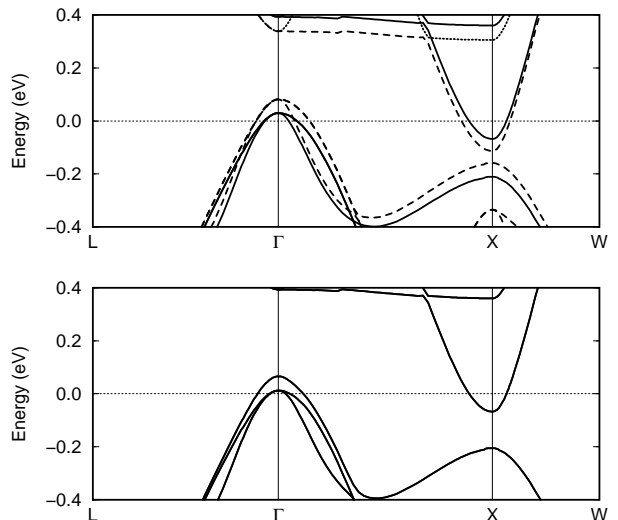


FIG. 4. Enlargement of the band structure of  $\text{Fe}_2\text{VAI}$  near the Fermi level. Upper panel shows how gradient corrections affect the band overlap (dashed lines show bands before gradient corrections are included), by shifting states at X. Both gradient corrections and spin-orbit coupling are included in the lower panel.

**Spin-Orbit Coupling.** The result of spin-orbit coupling is to split the triply degenerate  $\Gamma_{25'}$  band maximum of mostly Fe  $t_{2g}$  character into  $j = \frac{3}{2}$  and  $j = \frac{5}{2}$  levels separated by 56 meV. The lower doublet leads to a pair of hole pockets whose occupation is an order of magnitude less than that of the remaining hole pocket. The result is that the number of hole carriers is affected only little, but the “degeneracy” is lifted and the Fermi wavevector of the holes is increased by  $3^{1/3} \approx 1.4$ .

**Determination of Fermi Level.** To determine the position of the Fermi level, the hole pocket and the electron ellipsoids at X were fit along high symmetry directions to small wavevector expansions

$$\varepsilon_k = \varepsilon_o + \alpha k^2 + \beta k^4. \quad (1)$$

Since the  $k^4$  term is important even though the Fermi energy is small, effective masses do not describe the dispersion precisely. We obtain roughly  $m_h^* \approx 1.0-1.1m$  for the main hole pocket, and  $m_l^* = 0.8m$  and  $m_{tr}^* = 0.3-0.35m$  for the longitudinal and transverse electron masses at X. The band overlap is 130 meV, and compensation determines the Fermi levels of 70 meV for the large hole pocket and 60 meV for electrons (relative to their respective band edges). The DOSs of the various pockets are shown in Fig. 5.

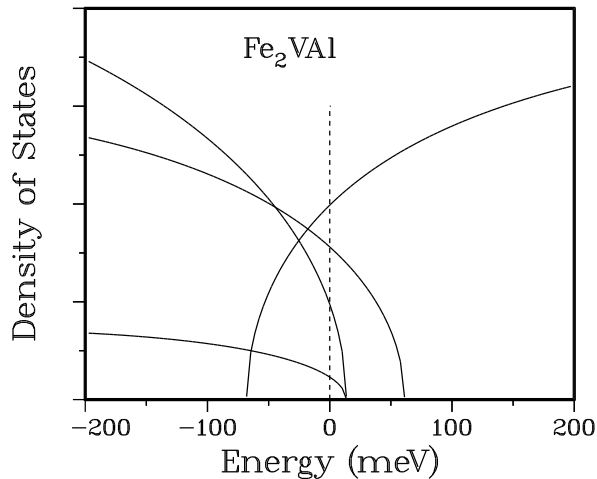


FIG. 5. Relative densities of states of the overlapping bands very near the Fermi level, from a small wavevector expansion discussed in the text. Two of the hole bands are nearly unoccupied and are neglected in the discussion in the text.

We finally obtain  $N(E_F) \approx 0.1$  states/eV, corresponding to a bare band specific heat coefficient  $\gamma_b \approx 0.2$  mJ/mole-K<sup>2</sup>. Compared to the extrapolated ( $T \rightarrow 0$ ) observed value [1] of 14 mJ/mole-K<sup>2</sup>, the apparent enhancement factor of the thermal mass is  $m_{th}/m_b \approx 70$ . We address this discrepancy in Sec. IV.

**Mechanical Properties and Effect of Pressure.** We calculated the energy for several crystal volumes. The lattice constant that minimizes the energy is 0.7% smaller than the experimental value ( $V/V_{obs}=0.98$ ). A fit to a polynomial gives a bulk modulus  $B=0.49$  Mbar. This indicates a relatively soft lattice, which can be compared to 1.7 Mbar for Fe and 0.7 Mbar for Al.

It will be of interest for future experiments what the effect of pressure on the band overlap of the semimetallic state is. From calculations at  $V=1.025 V_{obs}$  and  $V=0.95 V_{obs}$  which translates to a pressure difference of 36 Kbar, the change in band overlap is negligible. Hence we predict that the effect of even substantial pressure on the semimetallic state will be small.

### C. Magnetic Tendencies of Fe<sub>2</sub>VA1

We have checked for a ferromagnetic instability by performing fixed spin moment calculations. No such instability was found, consistent with the results of Singh and Mazin and also with expectations based on the very small value of  $N(E_F)$ , which would leave the system far from a Stoner instability. For small forced moments the V moment is parallel to that on the Fe ion and the energy *vs.* moment curve is parabolic. For total moment greater than  $0.3 \mu_B$ , however, the V moment becomes antiparallel and saturates around  $0.5 \mu_B$  as the Fe moments are driven to  $2 \mu_B$  and above. This behavior is plotted in

Fig. 6. In this range the energy *vs.* moment curve is linear.

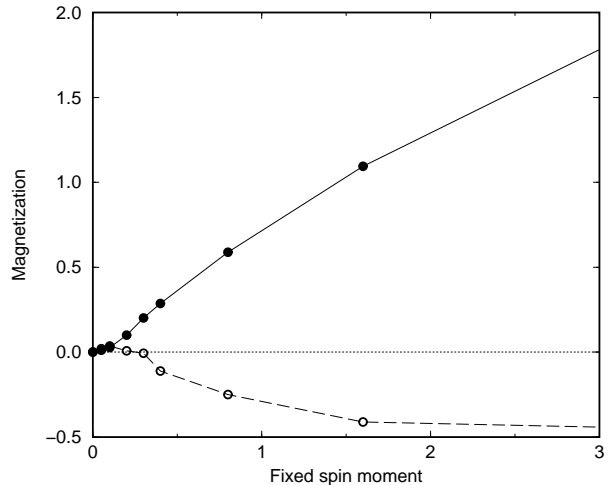


FIG. 6. Behavior of the moments on the Fe atom (solid dots) and on the V atom (open dots) when fixed spin moment calculations are carried out. Calculations were actually carried out for moments above  $3 \mu_B$  as well as for the points indicated.

A FM instability involves the  $\vec{q} = 0$  response of the system, which is weak due to the very small Fermi surfaces. The band structure contains more interesting low energy response at the zone boundary (X point) wavevector  $\vec{Q}_{100}=(1, 0, 0)2\pi/a$ , which could encourage an AF instability. This response arises from the intersection of the Fermi surfaces when the hole-derived surfaces at  $\Gamma$  are displaced by  $\vec{Q}_{100}$ . We searched for AF ordering of the simple cubic Fe sublattice, with cubic (rocksalt) ordering of Fe moments. The energy increases monotonically with Fe moment (arising from the imposed external staggered field  $H_{st}$ ) and no tendency toward instability was found. These results are consistent with the lack of any observed magnetic order.

### D. Characteristics of the Semimetallic State

The predicted carrier concentration is  $2.9 \times 10^{-3}$  carriers of each sign per formula unit (or one per  $350 \approx 7 \times 7 \times 7$  primitive cells). This number is four times smaller than that reported by Singh and Mazin due to the effect of the generalized gradient corrections to LDA, which push the electron band at X upward and thereby acts to decrease the band overlap and hence the carrier concentration. Since the electron carriers are V  $e_g$  character, they reside on the V sites which form an fcc lattice. The hole carriers are of primarily Fe  $t_{2g}$  character, and the Fe sites form a sc array of lattice constant  $\frac{a}{2}$ , on which the holes are an average of  $(350)^{1/3} \frac{a}{2} \approx 20 \text{ \AA}$  apart.

For qualitative purposes we can think in terms of a mass  $m_h^* \approx 1$  for holes with 1/700 of sites occupied, and mass  $m_e^* \approx 0.5$  of electrons with 1/350 of available sites occupied. Taking the Drude plasma frequencies as  $\Omega_p = 4\pi ne^2/m^*$  gives  $\hbar\Omega_p=70$  meV for the holes and 50 meV for the electrons.

### E. Importance of the Al Site

Singh and Mazin [7] have noted that the Al  $sp$  orbitals mix with the transition metal  $d$  states, with the result that little Al DOS remains in the vicinity of the Fermi level. Since isoelectronic  $\text{Fe}_2\text{VGa}$  has properties [3,4] similar to those of  $\text{Fe}_2\text{VAl}$ , we have carried out parallel calculations on the Ga compound at its lattice constant of 5.776 Å. [3,4] The resulting band structure is very similar. The (primarily Ga)  $s$  band centered 9.3 eV below  $E_F$  is 1 eV lower than the Al band in  $\text{Fe}_2\text{VAl}$ , but other differences are smaller. The band overlap giving rise to semimetallic character is 230 meV, compared to 130 meV in the Al compound. As a result, Fermi surface sizes and carrier concentrations are correspondingly larger than in  $\text{Fe}_2\text{VAl}$ .

To explore further the effect of the Al states, we calculated the band structure of the fictitious compound  $\text{Fe}_2\text{V}$  in which the Al atom is simply removed. Since this unit cell has an odd number of electrons, the electronic structure must differ qualitatively; it cannot be a paramagnetic semiconductor or be isomorphic to one (as the  $\text{Fe}_2\text{VAl}$  band structure is). The resulting band structure is shown in Fig. 7. The difference in the electronic structure is substantial, and is most obvious along the X-W direction.

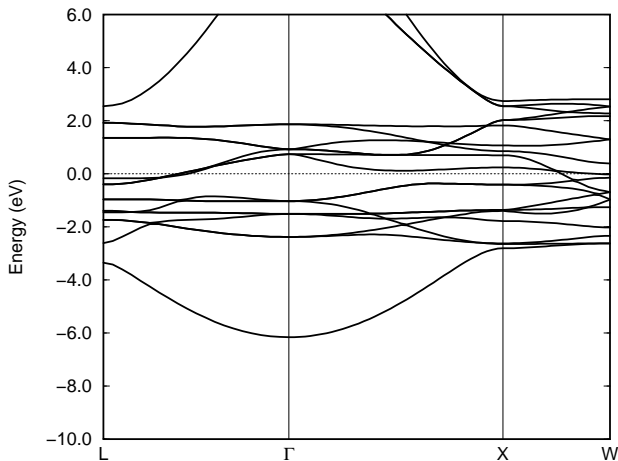


FIG. 7. Band structure of the fictitious compound  $\text{Fe}_2\text{V}$ , after the removal of the Al atom. The  $d$  bands narrow by at least 1.5 eV, and the band topology near the Fermi level rearranges.

The combined Fe-V  $d$  bands are considerably narrower, but corresponding bands can be located throughout the Brillouin zone and throughout the valence/conduction band energy range. This congruity of the band structures indicates that removal of Al is analogous to removing three valence electrons from the cell without removing bands (basis states available for occupation). As a result, there is  $d \rightarrow s$  charge promotion on both Fe and V as the lowest, primarily  $s$ -like, band changes from largely Al character to totally Fe and V character. The filling of the  $d$  bands drops, with an entire band along  $\Gamma$ -X-L becoming unoccupied and two bands along  $\Gamma$ -L becoming half empty. Relative band shifts are also substantial, and resulting change in band topology leads to the complete disappearance of the pseudogap due to band rearrangements at the W point. Thus the Al atom, or at least its three electrons, play a crucial rôle in determining the electronic behavior of  $\text{Fe}_2\text{VAl}$ . The active states at the Fermi level nevertheless have only a small amount of Al character, as emphasized by Singh and Mazin. [7]

### F. Doping on the V Sublattice

As an indication of the effect of replacing V with a heavier transition metal atom, a virtual crystal calculation was carried out for the case where the charge on the V nucleus, and the number of electrons, are increased by 0.5. This corresponds roughly to the case of  $\text{Fe}_2\text{V}_{1/2}\text{Cr}_{1/2}\text{Al}$ , or more roughly to  $\text{Fe}_2\text{V}_{5/6}\text{Fe}_{1/6}\text{Al}$ . The result is a ferrimagnetic state with a net moment near  $0.5 \mu_B$ , *i.e.* almost equal to the extra electronic charge in the cell. The band structure, shown in Fig. 8 in a region near the Fermi level, is severely disrupted near  $E_F$ , not resembling at all a situation in which the bands are rigidly split in a Stoner fashion. The convergence to a self-consistent solution was very slow, suggesting the FM state is not very stable. The net moment is derived from  $0.52 \mu_B$  within each Fe sphere and  $-0.45 \mu_B$  within the V sphere.

We have looked at the same doping level by doing a virtual calculation using the Al site, *i.e.* treating  $\text{Fe}_2\text{VAl}_{1/2}\text{Si}_{1/2}$ . Considering the behavior we found in Sec. III.E, that Al seems to simply dump its electrons into the system, this virtual crystal calculation may be a very realistic treatment of the Al-Si alloy. The result is very similar to doping on the V sublattice: the ferrimagnetic moment is again near  $0.5 \mu_B$ , with 0.42 on each Fe atom and -0.26 on each V atom. The differences between doping on the V and Al sublattices can be accounted almost entirely by the lowering of the V-derived electron bands when doping is done on the V site. We will report more of these results and a study of  $\text{Fe}_2\text{VSi}$  elsewhere.

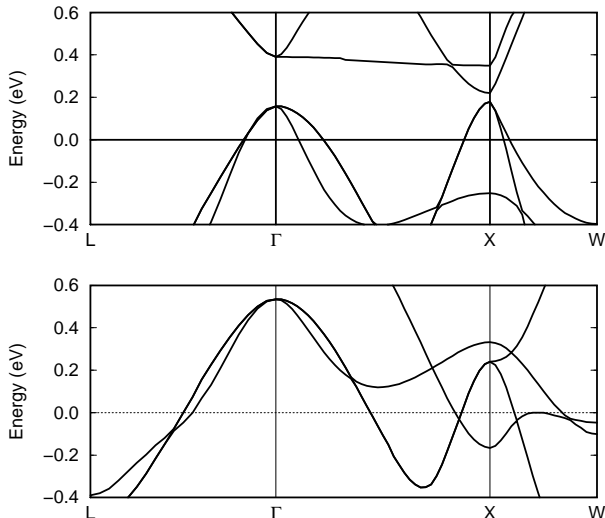


FIG. 8. Majority (a) and minority (b) band structures of the ferromagnetic state of the virtual crystal of  $\text{Fe}_2\text{V}_{1/2}\text{Cr}_{1/2}\text{Al}$ , illustrating the strong deviation from a simple Stoner splitting of the bands in this system.

#### IV. DISCUSSION OF EFFECTS OF INTERACTIONS

##### A. Excitonic Condensate?

The study of semiconducting or semimetallic systems in which the gap  $E_g$  (positive or negative) is very small has a long history, with residual interactions leading to the possibility of several exotic phases. A spontaneous condensed exciton phase is possible [13] when the gap  $E_g$  is less than the exciton binding energy  $E_B^x$ . The occurrence of the spontaneous excitonic phase in a narrow gap semiconductor or low density semimetal has been extensively studied and searched for experimentally, but only a few systems such as  $\text{TmSe}_{0.45}\text{Te}_{0.55}$  provide reasonable candidates for such a system. [14] Specific theoretical predictions are quite sensitive to the size and shape of the electron and hole Fermi surfaces. [15] The possibility of an exciton condensate in more highly correlated systems such as Kondo insulators has been suggested by Duan, Arovas, and Sham. [16]

The classic case of the group V semimetals lies at one extreme, where a one-electron picture works well and the effect of residual interactions is small. Bismuth is a compensated semimetal with less than  $10^{-5}$  electron and hole carriers per atom, yet it behaves at low temperature as a straightforward degenerate metal with observable (but tiny) Fermi surfaces. An intermediate case is represented by ScN, a rocksalt structure semimetal with a LDA band structure very much like that of  $\text{Fe}_2\text{VAl}$ : a calculated band overlap of 80 meV involving a threefold degenerate  $\Gamma_{15}$  hole pocket at  $\Gamma$  and electron ellipsoids at X. Monnier *et al.* [17] considered the additional correlation energy of

the electron and hole carriers within LDA and concluded that ScN remains semimetallic (*i.e.* an electron-hole liquid) with only modestly renormalized band overlap and effective masses.

The present case of  $\text{Fe}_2\text{VAl}$  has two new features not included in previous models. [13,15] First, the electrons and holes are well confined to distinct interpenetrating lattices so that the discreteness of the lattice may have an effect. Second, there are likely to be strong residual interactions. There will be repulsive electron-electron and hole-hole interactions, not only on-site but also intersite due to the weakness of the metallic screening. On-site exchange interactions on Fe and V may lead to magnetic fluctuations, although they should be much suppressed due to the low value of  $N(E_F)$ . Then there will be the attractive electron-hole interactions.

The response is described by the dielectric function  $\varepsilon = 1 - \hat{v}\chi_o$  where  $\hat{v}$  is a mean matrix element of the Coulomb interaction and the non-interacting susceptibility is

$$\chi_o(\vec{q}, \omega) = 2 \sum_{k,n,m} \frac{f(\varepsilon_{k,n}) - f(\varepsilon_{k+q,m})}{\varepsilon_{k+q,m} - \varepsilon_{k,n} - \hbar\omega}, \quad (2)$$

where  $\varepsilon_{k,n}$  is the band energy of band  $n$  and  $f(\varepsilon)$  is the Fermi-Dirac thermal occupation factor. For the band structure of  $\text{Fe}_2\text{VAl}$  there are three type of contributions at low energy  $\hbar\omega$ . For  $\vec{q} \rightarrow 0$  there is the usual repulsive intraband scattering (from holes and electrons separately) that gives rise to Drude absorption in the optical spectrum. This response corresponds to a Lindhard-like susceptibility from both the hole and electron pockets, with Drude plasma energies given in Sec. III.D. The characteristic Fermi wavelengths are of the order of  $\lambda_F \approx 12a = 70 \text{ \AA}$ .

Second, near the X point where  $\vec{q} = \vec{Q}_{100}$  and equivalent points there will be low  $\omega$  response as the  $\Gamma$ -centered hole Fermi surface displaced by  $\vec{Q}_{100}$  intersects one of the electron ellipsoid Fermi surfaces. Third, there will be low energy intervalley scattering of electrons centered at  $\vec{Q}_{110} = (1,0,0)\frac{2\pi}{a} - (0,-1,0)\frac{2\pi}{a}$  and symmetry-related vectors. In the fcc lattice  $\vec{Q}_{110}$  reduces to  $\vec{Q}_{100}$ . Thus attractive electron-hole scattering and intervalley repulsive electron-electron scattering occur at the same reduced wavevectors.

##### B. Excitonic Parameters

The scale factors describing the excitonic system [17] depend on the background dielectric constant  $\epsilon_\infty$  for the rigid lattice in the absence of carriers, and on the reduced mass  $\mu$  given by

$$\frac{1}{\mu} = \frac{1}{m_e^*} + \frac{1}{m_h^*}, \quad (3)$$

where the electron effective mass  $m_e^*$  is given by

$$\frac{3}{m_e^*} = \frac{1}{m_\ell} + \frac{2}{m_{tr}} \quad (4)$$

in terms of the longitudinal ( $m_\ell$ ) and transverse ( $m_{tr}$ ) masses of the electron ellipsoid. For the calculated bands we obtain  $\mu \approx \frac{1}{3}m$ . The density of electron-hole pairs corresponds to a (bare, see below) density parameter  $r_s=30$ . The dielectric constant is difficult to estimate. It involves dipole matrix elements between  $d$  bands, which vanish in the atomic limit (dipole transitions require  $p \rightarrow d$  or  $d \rightarrow f$  transitions in this limit). Moreover, the valence and conduction bands are dominated by Fe and V respectively, on two separate sublattices, which will tend to reduce matrix elements. Since the Fe and V  $d$  states retain much of their atomic character in this solid, we do not expect a large value of  $\epsilon_\infty$ .

The exciton radius  $a_B^x$ , effective Rydberg  $E_B^x$  (the binding energy), and density parameter  $r_s^x$  are given by [17]

$$a_B^x = \epsilon_\infty \frac{m}{\mu} a_B, \quad (5)$$

$$E_B^x = \frac{1}{\epsilon_\infty^2} \frac{\mu}{m} E_R, \quad (6)$$

and

$$r_s^x = \frac{a_B}{a_B^x} r_s = \frac{1}{\epsilon_\infty} \frac{\mu}{m} r_s, \quad (7)$$

where  $E_R$  is the Rydberg and  $a_B$  is the Bohr radius.

In Table I we provide values of these parameters for  $\epsilon_\infty = 2, 5, 10, \text{ and } 20$ . From the band structure and the band character we expect  $\epsilon_\infty$  to lie in the lower end of this range. In any case, however, the exciton radius is large and the resulting effective density parameter  $r_s^x$  is far from the low density range where an exciton condensate might be expected. Moreover, the Thomas-Fermi screening length for this density of electrons (or holes) is still  $\approx 2 \text{ \AA}$ , so screening is still a consideration. In any case, a true exciton condensate would be an insulator, which is not the case for the reported samples (unless the conduction is a result of defects). Thus an exciton condensate is not expected to arise. Moreover, since there is only a factor of two difference in masses, a hole Wigner crystal screened by the lighter electrons also is not a likely scenario. However, an electron-hole plasma of low density ( $r_s=30$ ) may have strong dynamic correlations, which we address next.

TABLE I. Values of the excitonic radius  $a_B^x$ , binding energy  $E_B^x$ , and density parameter  $r_s^x$  for representative values of  $\epsilon_\infty$ .

$\epsilon_\infty$	$a_B^x/a_B$	$E_B^x$ (meV)	$r_s^x$
2	6	1150	5
5	15	180	2
10	30	45	1
20	60	11	0.5

### C. Excitonic Correlations

An interaction that will be nearly unscreened in this system is the attraction between an electron on a V site and a hole on a neighboring Fe site. The V-Fe separation is only  $2.5 \text{ \AA}$ , and since the density of electrons and holes separately is in the vicinity (if  $\epsilon_\infty$  is small) of that where Wigner crystallization should occur, [18] a homogeneous screening approximation may have broken down anyway. We suggest that a Hamiltonian of the form

$$\begin{aligned} H = & \sum_{i,i',s,s'} t_{i,i'}^e e_{i,s}^\dagger e_{i',s'} + \sum_{j,j',s,s'} t_{j,j'}^h h_{j,s}^\dagger h_{j',s'} \\ & - V^{eh} \sum_{\langle i,j \rangle, s, s'} n_{i,s}^e n_{j,s'}^h \\ & + U^e \sum_i n_{i,+}^e n_{i,-}^e + U^h \sum_j n_{j,+}^h n_{j,-}^h \end{aligned} \quad (8)$$

includes the important residual interactions. Here  $e_{i,s}^\dagger$  creates an electron of spin  $s$  (equal to  $+$  or  $-$ ) on the  $i$ -th site of the V sublattice, and  $h_{j,s}^\dagger$  creates a hole of spin  $s$  on the  $j$ -th site of the Fe sublattice,  $n^e = e^\dagger e$  and similarly for the hole occupation operator. The constants  $V^{eh}$  and  $U^e, U^h$  represent the corresponding interactions confined here to on-site for like particles, or nearest neighbors for the electron-hole interaction. The hopping amplitudes  $t^e$  and  $t^h$  are determined so as to reproduce the dispersion seen in Fig. 4. The attractive  $e-h$  attraction  $V^{eh}$  might be of the order of

$$V^{eh} \geq \frac{e^2}{\epsilon_\infty r_{n.n.}} e^{-k_{TF} r_{n.n.}} = \frac{2.5eV}{\epsilon_\infty} \times 0.3 \approx 150 \text{ meV} \quad (9)$$

if  $\epsilon_\infty \approx 5$ , with the equality being applicable only if Thomas-Fermi screening is applicable. If both dielectric and Thomas-Fermi screening are inapplicable due to the short separation,  $V^{eh}$  could approach the 1-2 eV range.

Falicov and Kimball [19] considered such a model, but treated only the case of infinitely heavy holes and neglect of identical particle repulsion. They obtained an anomalous temperature dependence of the carrier concentration. Kasuya [20] has considered the possibility of Wigner crystallization of excitons in a related picture, and suggested that picture might be appropriate for rare earth pnictides such as LaSb. The situation presented by  $\text{Fe}_2\text{VAl}$  does not seem to fit well within either of these pictures.

Since we expect the kinetic energy to be sufficient to inhibit formation of bound excitons (as discussed in Sec. IV.B), dynamic correlations of excitonic character may be substantial. To account for the observed behavior, the interactions have to be large enough to keep the system from simply reverting to a degenerate metal (such as Bi). Two effects oppose formation of coherent propagating electron-hole pairs: the electrons and holes have different velocities (although very similar in magnitude), and they move on inequivalent sublattices. Nevertheless

excitonic correlations should occur and grow in strength as the temperature is lowered. These correlations result in neutral objects that do not carry current, hence the resistivity should increase at low temperature, as observed, as carriers are effectively removed in pairs from the conduction process. Whether the photoemission spectra and the thermal mass enhancement can be obtained will require further treatment of this model Hamiltonian, which will be presented elsewhere. This Hamiltonian would be expected to show superconductivity in its phase diagram as well, although perhaps not at very low density.

## V. SUMMARY

Within the local density approximation,  $\text{Fe}_2\text{VAl}$  is found to be a low density semimetal. It is not unstable toward magnetic ordering, in agreement with observation, although addition of rather small amounts of carriers produces ferromagnetism, as observed. The Al atom is found to have a strong but indirect effect on the electronic structure of this compound. The observed properties, including a heat capacity that is seventy times larger than the semimetallic DOS can account for, indicate that other processes are occurring in this system.

The density of electrons and holes is in the range where individually formation of a Wigner crystal is expected, and hence long-range interactions might be expected to be of importance. We have suggested rather that dynamic exciton-like short-range correlations (arising from short-range interactions) will dominate the observed behavior, and account for at least some of the enhancement of the thermal mass and for the upturn in the resistivity at low temperature. We have considered the possibility of an exciton condensate ground state, but for this picture to be viable, but even for an unreasonably small background dielectric constant a conventional condensate does not seem to be indicated. A two-band, extended Hubbard model with attractive electron-hole interaction has been suggested as a possible model to capture the essential processes, including excitonic correlations. The possibility of inhomogeneous magnetism, as suggested by Singh and Mazin, remains a possibility for accounting for some of the observed behavior.

## VI. ACKNOWLEDGMENTS

We are grateful to W. L. Lambrecht for bringing Ref. [17] to our attention. This work was supported by the U. S. Office of Naval Research.

- [1] Y. Nichino, M. Kato, S. Asano, K. Soda, M. Hayasaki, and U. Mizutani, Phys. Rev. Lett. **79**, 1909 (1997).
- [2] K. Endo, H. Matsuda, K. Ooiwa, and K. Itoh, J. Phys. Soc. Jpn. **64**, 2329 (1995).
- [3] K. Endo, H. Matsuda, K. Ooiwa, M. Iijima, K. Ito, T. Goto, and A. Ono, J. Phys. Soc. Jpn. **66**, 1257 (1997).
- [4] N. Kawamiya, Y. Nishino, M. Matsuo, and S. Asano, Phys. Rev. **B44**, 12406 (1991).
- [5] G. R. Stewart, Rev. Mod. Phys. **59**, 755 (1984).
- [6] D. E. Okpalugo, J. G. Booth, and C. A. Faunce, J. Phys. **F 15**, 681 (1985).
- [7] D. J. Singh and I. I. Mazin, cond-mat/9801302.
- [8] D. J. Singh, *Planewaves, Pseudopotentials, and the LAPW Method* (Kluwer Academic, Boston, 1994).
- [9] P. Blaha, K. Schwarz, and J. Luitz, WIEN97, Vienna University of Technology, 1997. Improved and updated version of the original copyrighted WIEN code, which was published by P. Blaha, K. Schwarz, P. Sorantin, and S. B. Trickey, Comput. Phys. Commun. **59**, 399 (1990).
- [10] S. H. Wei and H. Krakauer, Phys. Rev. Lett. **55**, 1200 (1985); D. J. Singh, Phys. Rev. **B 43**, 6388 (1991).
- [11] J. P. Perdew, J. A. Chevary, S. H. Vosko, K. A. Jackson, M. R. Pederson, and D. J. Singh, Phys. Rev. **B 46**, 6671 (1992); J. P. Perdew, K. Burke, and M. Ernzerhof, Phys. Rev. Lett. **77**, 3865 (1996).
- [12] A.H. MacDonald, W.E. Pickett and D.D. Koelling, J. Phys. **C13**, 2675 (1980).
- [13] B.I. Halperin and T. M. Rice, Rev. Mod. Phys. **40**, 756 (1968).
- [14] B. Bucher, P. Steiner, and P. Wachter, Phys. Rev. Lett. **67**, 2717 (1991).
- [15] Yu. V. KopaeV and T. T. Mnatsakanov, Fiz. Tverd. Tela **15**, 744 (1973) [Sov. Phys. Solid State **15**, 520 (1973)].
- [16] J.-M. Duan, D. P. Arovas, and L. J. Sham, Phys. Rev. Lett. **79**, 2097 (1997).
- [17] R. Monnier, J. Rhyner, T. M. Rice, and D. D. Koelling, Phys. Rev. **B31**, 5554 (1985).
- [18] H. B. Shore, E. Zaremba, J. H. Rose, and L. Sander, Phys. Rev. **B18**, 6506 (1978) find crystallization to occur around  $r_s=26$ .
- [19] L. M. Falicov and J. C. Kimball, Phys. Rev. Lett. **22**, 997 (1969).
- [20] T. Kasuya, J. Phys. Soc. Jpn. **61**, 2206 (1992).